doi.org/10.36721/PJPS.2026.39.12.339.1

Rapid analysis of the chemical composition of the *Equiseti hiemalis herba* based on UHPLC-Q-Exactive Orbitrap MS with parallel reaction monitoring

Qing Li[1,2#], Pei Xiong[3#], Min Zhang[2], Kaiquan Yu[2], Jiaxin Li[2] and Hui Li[2]*

[1]School of Pharmacy, Baotou Medical College, Baotou 014000, China
[2]School of Pharmaceutical Science, Sino-Pakistan Center on Traditional Chinese Medicine, Hunan University of Medicine, Huaihua, Hunan 418000, People's Republic of China
[3]School of Pharmacy, Nanjing University of Traditional Chinese Medicine, Nanjing, Jiangsu 210023, People's Republic of China

Abstract: **Background**: *Equiseti hiemalis herba* (EH) is traditionally used for heat-clearing, promoting diuresis, resolving phlegm, relieving cough, improving vision and reducing ocular opacity. Previous phytochemical studies on EH have mainly focused on flavonoids and organic acids, whereas a comprehensive characterization of its chemical constituents remains lacking. **Objectives**: This study aimed to establish a rapid and systematic analytical strategy for the comprehensive characterization of chemical constituents in EH. **Methods**: In this work, a UHPLC-Q-Exactive Orbitrap MS system was employed for compound identification, utilizing full MS scan with subsequent data-dependent MS^2 acquisition or parallel reaction monitoring incorporating an inclusion ion list. **Results**: A total of 82 compounds were identified or tentatively characterized from EH, including 34 organic acids, 22 flavonoids, 10 terpenes, 3 nucleotides, 3 amino acids, 3 coumarins, 2 alkaloids and 5 other compounds. Among them, 71 compounds were reported in EH for the first time. Organic acids and flavonoids were the predominant constituents, while the identification of terpenes further revealed the chemical diversity of EH. **Conclusion**: The established analytical strategy provides an effective approach for the rapid characterization of chemical constituents in EH and offers a theoretical basis for further studies on its pharmacodynamic material basis and pharmacological mechanisms.

Keywords: *Equiseti Hyemalis Herba*; Identification; Organic acids; Parallel reaction monitoring; UHPLC-MS

Submitted on 07-03-2024 – Revised on 29-05-2026 – Accepted on 15-06-2026

INTRODUCTION

Equiseti hiemalis herba (EH), the dried aerial part of *Equisetum hiemale* L., is a perennial herbaceous plant characterized by hollow, cylindrical and jointed stems without obvious branching (Chinese Pharmacopoeia Commission, 2025). EH is widely distributed in several provinces of China, including Hunan, Heilongjiang, Jilin, Liaoning and Hebei, as well as neighboring regions (Editorial Committee of flora of China, 2004).

EH has traditionally served as a medicinal plant in China and exhibits a broad spectrum of therapeutic effects, including heat-clearing, promoting diuresis, resolving phlegm, relieving cough, improving vision and reducing ocular opacity (Chinese Pharmacopoeia Commission, 2025). It has also been widely applied in the management of eye diseases, gastrointestinal bleeding, dysentery, liver prolapse and malaria (Nicolau *et al*., 2023; Zhang *et al*., 2025). Previous chemical studies indicated that EH contains diverse classes of chemical constituents, including flavonoids, organic acids, alkaloids and volatile oils (Ma and Zhou, 2025). Among them, flavonoids and phenolic acids are regarded as the principal active components. Recent studies further suggested that EH possesses multiple biological activities, such as antihypertensive, analgesic, hemostatic and diuretic effects (Boeing *et al*., 2021; Wu *et al*., 2025). For example, ferulic acid, an important phenolic acid component in Equisetaceae plants, has been reported to exert analgesic activity by inhibiting platelet aggregation and suppressing the release of 5-hydroxytryptamine from platlets (Ataseven *et al*., 2021; Dong and Huang, 2022). In addition, cinnamic acid and its derivatives possess multiple biological properties, including antibacterial, enzyme inhibitory and antitumor activities (Xu *et al*. 2013). Gallocatechin, a representative flavonoid constituent, has likewise been shown to exhibit anti-inflammatory, antiviral and anticancer activities (Ciesek *et al*. 2011; Gomes *et al*. 2018; Venkatakrishnan *et al*. 2018).

UHPLC-MS/MS has been widely recognized as an efficient analytical platform for the characterization of chemical constituents in herbal medicines, pharmaceutical preparations and biological matrices (Cai *et al*., 2020; Hu *et al*., 2020; Ren *et al*., 2020). This approach integrates the exceptional resolution of UHPLC with the high sensitivity afforded by MS. The ability to identify molecular structures by providing rich mass-spectral fragmentation information enables more accurate

**Corresponding author:* e-mail: lhi18@163.com
#These authors contributed equally and are the co-first authors.

structural inference of unknown compounds (Liao *et al*., 2021; Luo *et al*., 2026). However, a full MS scan cannot obtain MS2 spectra for all compounds, preventing identification of compounds in trace amounts. Parallel reaction monitoring (PRM), combined with the inclusion ion list technique, is a new MS scan mode based on a designated ion list containing precursor ions, thereby obtaining all fragment information of the target compound (Zhang *et al*., 2022; Zhang *et al*., 2023). Accordingly, a comprehensive, in-depth exploration of the unknown chemical components in EH is required. In the present study, UHPLC-Q-Exactive Orbitrap MS was employed to rapidly and reliably characterize the chemical constituents in EH, which may provide a theoretical basis for further studies of its pharmacodynamic basis and pharmacological mechanisms.

MATERIALS AND METHODS

Apparatus and supplies

Instruments

UHPLC-MS/MS characterization was performed using a Q-Exactive Focus Orbitrap mass spectrometer (Thermo Electron, Bremen, Germany) coupled with a Thermo Scientific Dionex Ultimate 3000 RS UHPLC system (Thermo Fisher Scientific, California, USA) through an electrospray ionization (ESI) interface. An ultrasonic cleaner, purchased from Kunshan Ultrasonic Instruments Co., Ltd. (Kunshan, China), was used for sample preparation. An electronic balance (AUY120, Shimadzu Corporation, Japan) served for weighing all reagents and samples.

Chemicals and reagents

HPLC-grade methanol, acetonitrile and formic acid were supplied by Fisher Scientific (New Jersey, USA). Distilled water was provided by Guangzhou Watsons Food and Beverage Co., Ltd. (Guangzhou, China). Citric acid (batch no. C108869) was acquired from Tianjin Zhiyuan Chemical Reagent Co., Ltd. (Tianjin, China). Suberic acid (batch no. 20190620), 4-hydroxybenzoic acid (batch no. DH1925000) and ferulic acid (batch no. UD 3365500) were provided by West Asia Chemical Technology (Shandong) Co., Ltd. (Shandong, China). Quercetin (batch no. AF804180) was obtained from Chengdu Alfa Biotechnology Co., Ltd. (Chengdu, China). Three reference compounds-namely isoquercitrin (batch no. Y-076-181025), kaempferol-7-O-β-D-glucopyranoside (batch no. RFS-S10602201020) and kaempferol (batch no. S-014-171216) were provided by Chengdu Herbpurify Co., Ltd., located in Chengdu, China. Phlorizin (batch no. wkq18050407) was supplied by Sichuan Weiqi Biotechnology Co., Ltd. (Sichuan, China). The reagents used had a purity exceeding 98%.

The specimen of EH was collected in Yingkou Town, Hecheng District, Huaihua City, Hunan Province and its taxonomic identity was later confirmed by Professor Cai Wei at Hunan University of Medicine. The collected materials were oven-dried at 60°C before further analysis.

Methods

UHPLC apparatus and parameters

A Thermo Scientific Hypersil GOLD^{TM} aQ column (100 mm × 2.1 mm, 1.9 μm) was employed for chromatographic separation. The mobile phase consisted of 0.1% formic acid aqueous solution (A) and acetonitrile (B), delivered at a flow rate of 0.3 mL/min. The elution gradient was programmed as follows: 95% A at 0 min, 90% A at 2 min, 80% A at 5 min, 75% A at 10 min, 45% A at 12 min, 20% A at 20 min, 5% A at 25 min, followed by re-equilibration to 95% A at 26 min and maintained until 30 min. The injection volume was 2 μL and the column temperature was 40ºC.

Mass spectrometry instrumentation and conditions

The Q-Exactive Focus Orbitrap MS system was hyphenated to the UHPLC equipped with an ESI interface. The spray voltage was set to 3.5 kV in positive ionization mode and 3.0 kV in negative ionization mode. The other instrument conditions for the positive- and negative-ion modes were the same. The sheath gas and auxiliary gas were set to 30 and 10 arbs, respectively, while the capillary temperature, auxiliary heater temperature, and S-lens RF level were fixed at 320ºC, 350ºC and 50ºC, respectively. High-resolution mass spectrometry was obtained at a resolution of 70000 in full-scan mode, with a scan range of m/z 120-1000 and MS/MS at a resolution of 17500. Mass spectral data were collected using either full MS-ddMS^2 or PRM acquisition modes. In addition, the databases used in this study included mzVault, mzCloud, Massbank and Orbitrap Traditional Chinese Medicine Library (OTCML).

Preparation of the EH extracts

1.0 g of dried EH sample was precisely weighed and transferred into a 50 mL conical flask, then 20 mL of 70% methanol-water solution was added. Ultrasonic-assisted extraction was performed for 1 h to promote the dissolution of target constituents. Thereafter, the obtained extract was passed through a 0.22 μm membrane filter to eliminate insoluble particles and the resulting filtrate was collected for LC-MS analysis.

Preparation of standard solutions

The standard solution of 0.1 mg/mL was obtained by dissolving appropriate amounts of 4-hydroxybenzoic acid, ferulic acid, quercetin, isoquercitrin, suberic acid, citric acid, kaempferol, phlorizin and kaempferol-7-O-β-D-glucopyranoside in methanol, respectively and stored at 4°C for later use.

RESULTS

Analytical method

A systematic UHPLC-HRMS-based strategy was developed for the detailed profiling of the chemical constituents in EH. To achieve optimal chromatographic separation, several critical parameters were systematically investigated during method development, including extraction solvents (60%, 70% and 80% methanol), mobile phase compositions (methanol-0.1% formic acid aqueous solution and acetonitrile-0.1% formic acid aqueous solution), gradient elution procedures and column temperatures (40°C and 45°C). The results demonstrated that the optimal separation performance was achieved using 70% methanol as the extraction solvent, acetonitrile with 0.1% formic acid aqueous solution as the mobile phase, a column temperature of 40°C and an optimized gradient elution program.

Under the optimized conditions, the samples underwent ultrasonic extraction prior to analysis using a Q-Exactive Focus Orbitrap MS coupled to UHPLC in full-scan mode. Potential chemical constituents were preliminarily screened using Compound Discoverer 3.0 software integrated with a metabolite analysis workflow. Subsequently, comprehensive mass spectrometric and tandem mass spectrometric data were acquired via full-scan analysis combined with PRM, using an inclusion ion list, to obtain detailed fragmentation information. PRM enabled the selective targeting and confirmation of precursor ions, thereby improving the reliability of compound identification, particularly for low-abundance isomers and trace constituents. Finally, the compounds were accurately or tentatively identified according to diagnostic fragment ions, retention times, an in-house database and relevant literature reports.

Identification of chemical composition

The extracting solutions of the EH were analyzed using a Thermo UHPLC-Q-Exactive Orbitrap MS according to the detection conditions under "2.1". The detection of 82 compounds under positive and negative ion scanning modes resulted in 71 Compounds being identified from EH for the first time. Representative high-resolution extracted ion chromatograms (EICs) in both positive and negative ion modes, together with the base peak chromatograms (BPCs), are presented in figure 1. Detailed in table S1 are the measured and calculated parameters for every compound, such as retention time, precursor ion *m/z* values and MS/MS fragmentation data.

Nucleotides

Negatively charged ions are formed during mass spectrometry when nucleotides, which contain phosphate and ribose groups, undergo loss of ribose (Wilfried and Ricardo, 2017).

Compounds 2 and 7 were detected at retention times of 0.96 and 1.26 min, respectively and shared the precise molecular formula $C_{10}H_{13}N_5O_4$. Both compounds exhibited a protonated molecular ion at *m/z* 268.104 $[M+H]^+$ together with a characteristic fragment ion at *m/z* 136.0619 $[M+H\text{-ara}]^+$ and it is speculated that they were isomers of adenosine based on the database.

At a retention time of 1.15 min, peak 6 exhibited a $[M+H]^+$ ion at *m/z* 136.0620, along with characteristic fragment ions at *m/z* 119.0356 $[M+H\text{-}NH_2]^+$ and 94.0405 $[M+H\text{-}CHN_2]^+$. Based on the literature, this peak was tentatively assigned as adenine (Li *et al*., 2026).

Amino acids

Amino acids mainly undergo protonation and carbon skeleton breakage in mass spectrometry. During the process of carbon skeleton fracture, the carbon-oxygen bonds in amino acid ions break, producing a series of fragment ions, such as -NH_2, -COOH and H_2O, as well as side-chain cleavage reactions (Choi *et al*., 2013; Li *et al*., 2024).

Compound 8 was produced as a protonated ion at *m/z* 132.1021 $[M+H]^+$ and a characteristic fragment ion at *m/z* 86.0870 $[M+H\text{-}CH_2O_2]^+$ at a retention time of 1.31 min, which was tentatively assigned as leucine based on literature comparison (Xiong *et al*., 2023).

The retention time of peak 12 was 1.84 min and the precise molecular formula was $C_9H_{11}NO_2$, detected as quasi-molecular ion at *m/z* 166.0864 $[M+H]^+$ and obtained MS^2 fragmentation ion at *m/z* 120.0810 $[M+H\text{-}CHO_2]^+$ and was deduced as L-Phenylalanine in line with literature (Xiong *et al*., 2023).

Peak 16 appeared at 3.20 min and generated $[M+H]^+$ ions at *m/z* 205.0973, producing fragment ions at *m/z* 188.0706 $[M+H\text{-}NH_2]^+$ and 146.0601 $[M+H\text{-}NH_2\text{-}C_2H_2O]^+$. So compound 16 was putatively identified as tryptophan (Li *et al*., 2023).

Flavonoids

A total of 22 flavonoids were identified in EH. Flavonoids are a class of compounds characterized by a 2-phenyl chromone skeleton. Flavonoid compounds predominantly undergo retro-Diels-Alder (RDA) cleavage, as well as reactions involving the removal of functional groups such as CO, CO_2 and H_2O and rearrangement reactions. And flavonoid glycosides are prone to successive removal of neutral fragments such as glucoside (162 Da), sophoroside (324 Da) and CO (28 Da) (He *et al*., 2017; Jiang and Gates, 2024).

Compounds 60, 61, 63, 65 and 70 were characterized as isoquercitrin, quercetin, kaempferol-7-O-β-D-glucopyranoside, phlorizin and kaempferol by comparing their retention times and MS spectra with those of the standards. The fragmentation pathways of quercetin and phlorizin are illustrated in figure 2A and 2B, respectively.

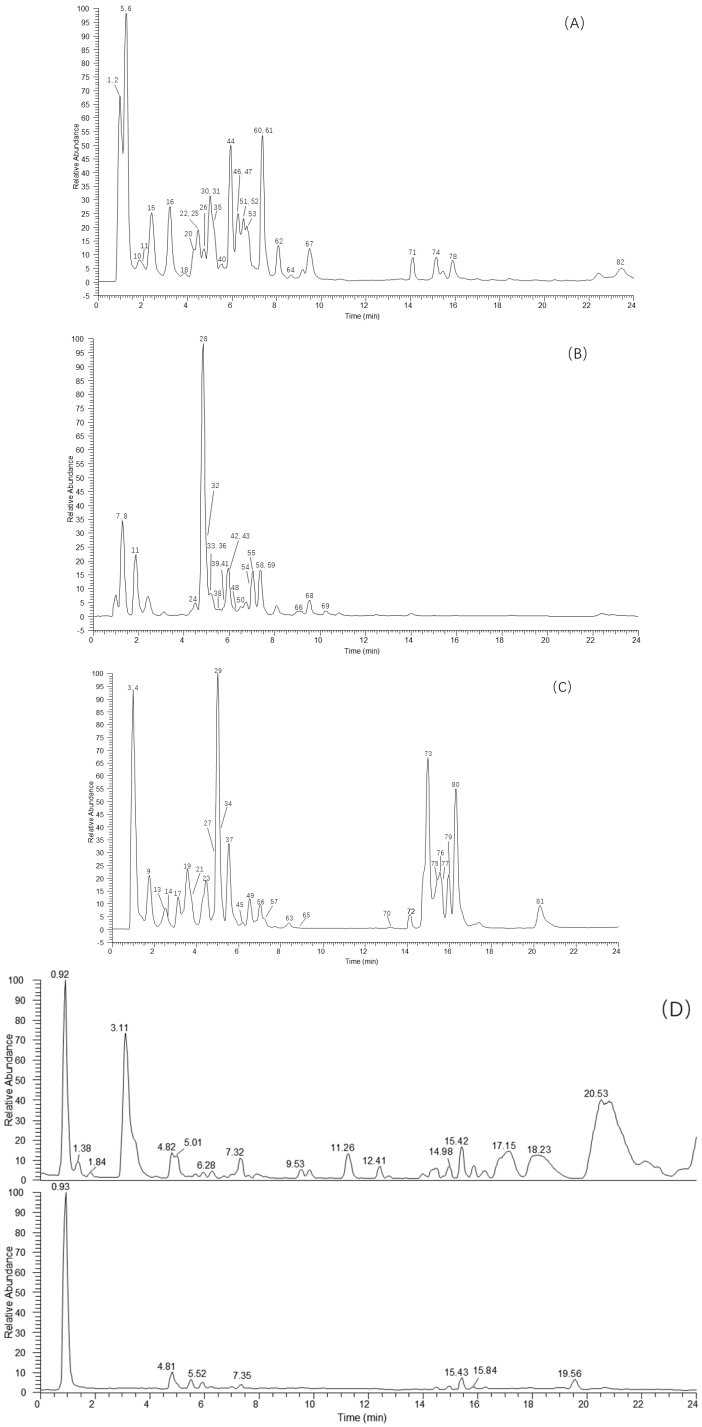

Fig. 1: High-resolution extracted ion chromatograms (EICs) and base peak chromatograms (BPCs) of EH. (A and B) Representative EICs obtained in positive ion mode with *m/z* values of (A) 149.05970, 163.07535, 303.04992, 409.14930, 433.11292, 465.10275, 627.15557, 127.03897, 136.06177, 144.10190, 177.05462, 205.09715, 209.15360, 219.17434, 268.10403, 277.17982, 307.08122, 310.24890, 425.37779, 447.09218 and 525.16026 and (B) *m/z* 535.21738, 132.10190, 166.08625, 193.15869, 197.11722, 209.15360, 268.10403, 611.16066, 627.15557, 773.21348 and 789.20839; (C) Representative EICs obtained in negative ion mode with *m/z* values of 133.01424, 191.01972, 315.07215, 329.08780, 153.01933, 137.02441, 339.07215, 311.04085, 355.10345, 341.08780, 625.14102, 163.04006, 193.05063, 407.09837, 447.09328, 435.12967, 285.04046, 293.17583, 721.36520, 697.36520, 293.21221, 723.38085, 699.38085, 279.23295 and 173.08193; (D) BPCs of EH in positive and negative ion modes, displayed from top to bottom, respectively.

Compound 47 showed the identical quasi-molecular ion at *m/z* 465.103 $[M+H]^+$ with compound 60, yielding fragmentation at *m/z* 303.0500 $[M+H\text{-glc}]^+$, which hinted at the presence of an isoquercitrin moiety. Thus, they were tentatively identified as isoquercitrin isomers. Likewise, compounds 22, 24, 33, 34, 38, 44 and 48 presented the precursor ions at *m/z* 465.1030 (0.66 ppm, $C_{21}H_{21}O_{12}$), 789.2089 (0.66 ppm, $C_{33}H_{39}O_{22}$), 789.2088 (0.51 ppm, $C_{33}H_{39}O_{22}$), 625.1413 (0.54 ppm, $C_{33}H_{41}O_{22}$), 627.1561 (0.88 ppm, $C_{27}H_{31}O_{17}$), 627.1563 (1.26 ppm, $C_{27}H_{31}O_{17}$) and 627.1560 (0.88 ppm, $C_{27}H_{31}O_{17}$), respectively, sharing the same fragment ion at *m/z* 303.049 ($C_{15}H_{11}O_7$), indicative of a quercitrin moiety and were thus preliminarily identified as quercetin-4'-O-glucoside (Ma *et al*., 2022), quercetin-glucose-gentiobioside isomer, quercetin-glucose-gentiobioside isomer (Wang *et al*., 2022), quercetin-3,4'-O-di-beta-glucopyranoside, quercetin-diglucoside isomer, quercetin-diglucoside isomer and quercetin-diglucoside isomer (Sánchez-Rabaneda *et al*., 2004), respectively.

Compounds 28, 41 and 55 signaled the precursor ions at *m/z* 773.2121 (-1.71 ppm, $C_{33}H_{41}O_{21}$), 611.1604 (-0.33 ppm, $C_{27}H_{31}O_{16}$) and 611.1601 (-0.82 ppm, $C_{27}H_{31}O_{16}$), respectively and yielded the same fragment ion at *m/z* 287.054 ($C_{15}H_{11}O_6$), which suggested the presence of the kaempferol moiety. Therefore, they were putatively identified as kaempferol-sophoroside-glucoside (Sánchez-Rabaneda *et al*., 2004), kaempferol-sophoroside isomer and kaempferol-sophoroside isomer (Guijarro-Díez *et al*., 2015).

Compound 46, with a molecular formula of $C_{21}H_{19}O_{11}$, displayed a $[M+H]^+$ ion at *m/z* 447.0900 and fragment ions at *m/z* 285.0367 and 123.0441, corresponding to the losses of a glucosyl moiety and subsequent $C_8H_2O_4$, respectively. Based on comparison with literature (Wang *et al*., 2020), it was tentatively assigned as trihydroxyflavone-glucuronide.

Compound 57 was eluted at 7.23 min,displaying the quasi-molecular ion at $[M-H]^-$ at *m/z* 407.0985 ($C_{19}H_{19}O_{10}$) along with the fragment ion $[M-H]^-$ at *m/z* 245.0452 $[M-H\text{-glc}]^-$ and 244.0357 $[M-H\text{-glc-H}]^-$. This compound was tentatively identified as iriflophenone-2-O-β-glucoside in the light of the literature (Xie *et al*., 2014).

The peak time of compound 64 was 8.64 min and the exact molecular formula was $C_{21}H_{20}O_{10}$. Quasi-ionic peak was obtained at *m/z* 433.1132 $[M+H]^+$ and fragment ions at *m/z* 313.0698 $[M+H\text{-}C_4H_8O_4]^+$, 397.0907 $[M+H\text{-}2H_2O]^+$, 283.0549 $[M+H\text{-}C_5H_{10}O_5]^+$, which was presumed to be vitexin when compared with literature (Jiang *et al*., 2018).

The peak times for compounds 66, 68 and 69 were 8.97, 9.50 and 10.25 min, respectively, with the exact molecular formula $C_{27}H_{34}O_{11}$, all sharing a quasi-molecular ion at *m/z* 535.215 $[M+H]^+$ and fragment ions at *m/z* 491.225 $[M+H\text{-}CO_2]^+$, 449.214 $[M+H\text{-}CO_2\text{-acetyl}]^+$ and 287.161 $[M+H\text{-CO2-acetyl-glc}]^+$, which in conjunction with literature (Yang *et al*., 2017) were presumed to be 3,4,7-Trihydroxy-5-methoxy-8-prenylflavan-7-O-beta-D-glucopyranoside isomers.

Organic acids

A total of 34 organic acids were identified in EH. Organic acids are prone to undergo α- and β-fragmentation in mass spectrometry, including decarboxylation. α-fracture usually occurs at the carboxyl group α-C, and stable negative ions are generated from the molecular ions. β-Fracture usually occurs at the carboxyl group β-C and unstable negative ions are generated (Bowie *et al*., 2002). Compounds 4, 17, 45 and 56 were unambiguously identified as citric acid, 4-hydroxybenzoic acid, suberic acid and ferulic acid through comparison of retention time and MS^2 spect against authentic standards. The fragmentation routes of 4-hydroxybenzoic acid and ferulic acid are displayed in figure 3A and 3B, respectively.

Compounds 23 and 29 exhibited an identical deprotonated ion at *m/z* 355.1036 $[M-H]^-$, yielding fragment ions at *m/z* 178.0263 $[M-H\text{-glc-}CH_3]^-$ and 134.0362 $[M-H\text{-glc-}CH_3\text{-}CO_2]^-$, indicative of glucose loss. Hence, they were assigned as ferulic acid-O-glucose isomers (Cai *et al*., 2020).

Compound 9 gave a deprotonated molecular ion $[M-H]^-$ at *m/z* 315.0724, matching the molecular formula $C_{20}H_{18}O_{11}$ with a mass error of 0.93 ppm, along with a fragment ion at *m/z* 153.0183 corresponding to loss of a glucosyl moiety. Therefore, based on the literature, this compound was identified as protocatechuic acid-3-O-glucose (Zheng *et al*., 2020). Peak 13 eluted at 2.48 min and displayed an $[M-H]^-$ ion at *m/z* 329.0878. Its MS/MS fragments at *m/z* 167.0341 $[M-H\text{-glc}]^-$, 152.0105 $[M-H\text{-glc-CH}]^-$ and 123.0440 $[M-H\text{-glc-}CO_2]^-$, led to its tentative assignment as vanillic acid-O-glucopyranoside through comparison with literature (Sun *et al*., 2015).

Compounds 3 and 37 showed a similar molecular ion $[M-H]^-$ with *m/z* 133.0131 (-3.70 ppm, $C_4H_5O_5$) and a fragment ion at *m/z* 115.0025 $[M-H\text{-}H_2O]^-$ at retention times of 0.98 min and 5.52 min, respectively. They were identified as malic acid by comparing with the databases and literature (Li *et al*., 2026). Since the references indicated that L-malic acid eluted before D-malic acid, compound 3 was tentatively assigned as L-malic acid and compound 37 as D-malic acid (Onozato *et al*., 2022; Shu *et al*., 2025).

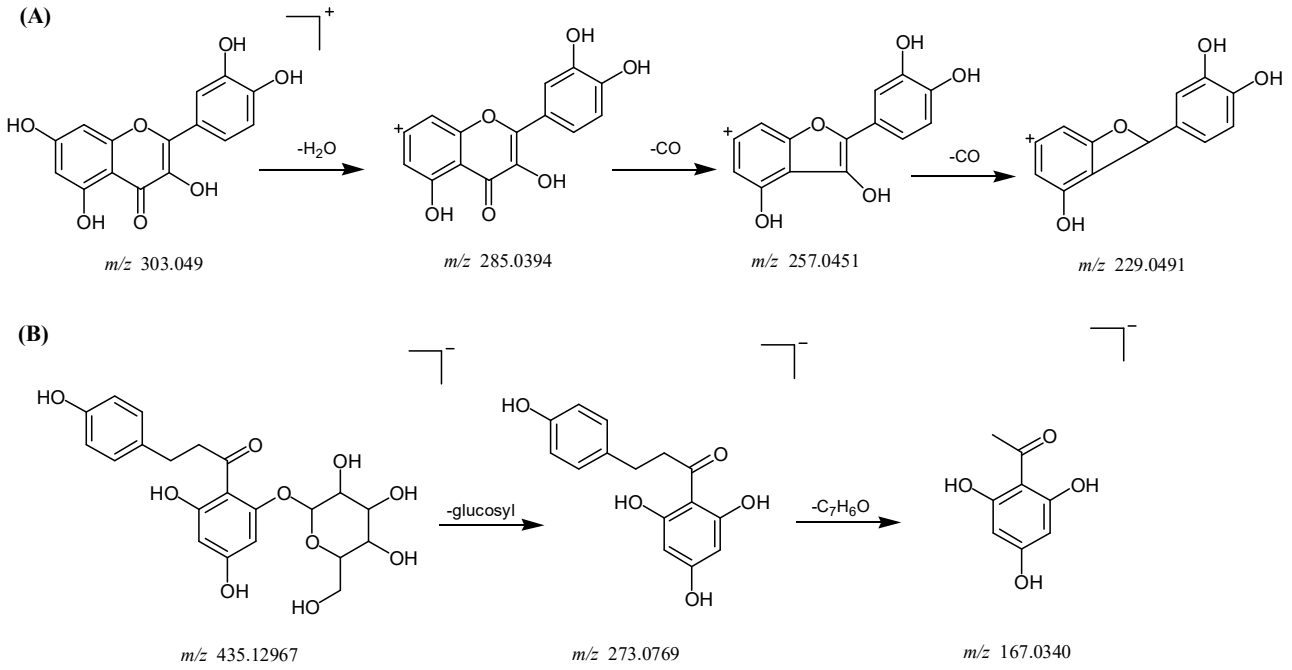

Fig. 2: Proposed mass spectrometric fragmentation pathways of (A) quercetin and (B) phlorizin.

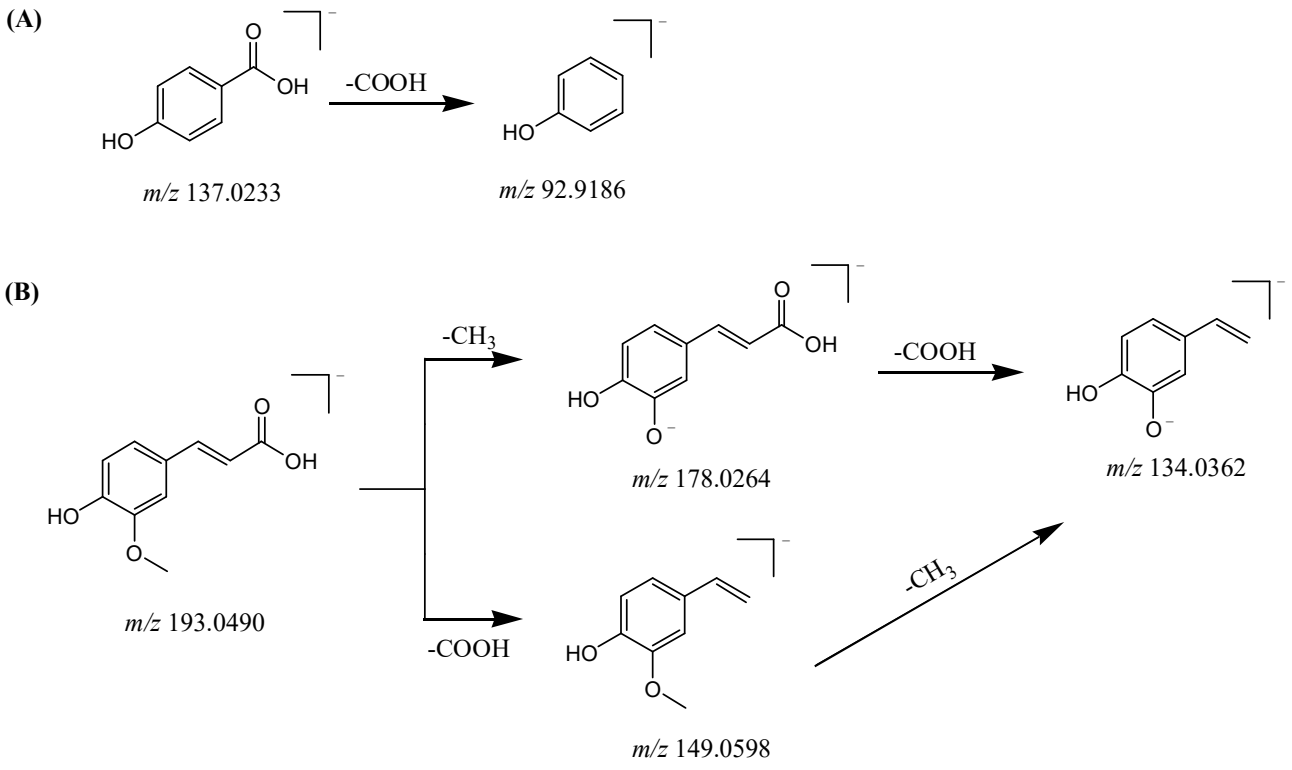

Fig. 3: Proposed mass spectrometric fragmentation pathways of (A) 4-hydroxybenzoic acid and (B) ferulic acid.

Compound 1 had a retention time of 0.94 min and an accurate molecular formula of $C_6H_6O_3$, with a quasi-molecular ion at *m/z* 127.0390 $[M+H]^+$, yielding a fragment ion at *m/z* 109.0288 $[M+H-H_2O]^+$, which was identified as pyrogallol in conjunction with the literature (Chen *et al*., 2019).

The retention times of compounds 11, 15, 18, 26 and 30 were 1.84 min, 2.99 min, 3.72 min, 4.71 min and 5.01 min, respectively. All had the exact molecular formula $C_9H_8O_2$, and all yielded quasi-ionic peaks at *m/z* 149.059 $[M+H]^+$ and fragment ions at *m/z* 103.0544 $[M+H-CO_2]^+$, 131.0661 $[M+H-OH]^+$ and 121.0283 $[M+H-C_2H_2]^+$,

which were presumed to be isomers of cinnamic acid in conjunction with literature (Wu *et al*., 2019). Compounds 20, 35, 40 and 50 (t_R 4.27, 5.23, 5.71, 6.56 min; $C_{10}H_{10}O_2$) each showed an $[M+H]^+$ at *m/z* 163.0751 with identical fragments at *m/z* 103.054 $[M+H-C_2H_4O_2]^+$ and 95.049 $[M+H-C_2H_4O_2-H_2O]^+$, suggesting methyl cinnamate isomers. Compound 49 (t_R 6.55 min) showed a deprotonated ion at *m/z* 163.0391 $[M-H]^-$ and a fragment at *m/z* 119.0490 $[M-H-CO_2]^-$, putatively identified as 4-hydroxycinnamic acid.

Compound 14 showed a deprotonated ion at *m/z* 153.0183 $[M-H]^-$ and a fragment ion at *m/z* 109.0283 $[M-H-CO_2]^-$ at a retention time of 2.55 min. It was based on the database. which was putatively identified as 3,4-Dihydroxybenzoic acid.

Compound 21 showed a deprotonated $[M-H]^-$ at *m/z* 311.0411 (0.81 ppm, $C_{13}H_{11}O_9$) and daughter ions at *m/z* 179.0342 $[M-H-ara]^-$, 149.0598 $[C_4H_5O_6]^-$ and 135.0441 $[M-H-ara-CO_2]^-$, resulting from loss of the arabinose moiety. It which was tentatively assigned as caftaric acid.

Compound 27 eluted at 4.81 min and showed a deprotonated ion $[M-H]^-$ at *m/z* 341.0884, consistent with the molecular formula $C_{15}H_{17}O_9$ (mass error 1.77 ppm). The MS/MS fragment ions at *m/z* 179.0341 and 135.0440 corresponded $[M-H-glc]^-$ and $[M-H-glc-CO_2]^-$, respectively. Thus, compound 27 was provisionally designated as CA-hexoside (Cai *et al*., 2020).

Compound 67 was eluted at 9.43 min, displaying a $[M+H]^+$ quasi-molecular ion at *m/z* 307.0812 (0.03 ppm, $C_{15}H_{14}O_7$) along with fragment ions at *m/z* 177.0548 $[M+H-C_5H_6O_4]^+$, 163.0390 $[M+H-C_6H_8O_4]^+$, and 150.0678 $[M+H-C_6H_5O_5]^+$. Literature identification as gallocatechin (Jaiswal *et al*., 2012).

Compounds 71 and 74 (t_R 14.11, 15.15 min; $C_{17}H_{24}O_3$) each showed an $[M+H]^+$ at *m/z* 277.179 and a common fragment at *m/z* 137.0599 $[M+H-C_9H_{16}O]^+$ and were identified as shogaol isomers (Wang *et al*., 2023). Likewise, compound 72 was putatively identified as gingerol.

Peak 76 gave a $[M-H]^-$ ion at *m/z* 293.2124 upon elution, with additional characteristic fragments at *m/z* 275.2018 $[M-H-H_2O]^-$, 235.102 $[M-H-C_3H_6O]^-$, 183.1383 $[M-H-C_3H_6O-C_4H_4]^-$ and 121.1012 $[M-H-C_3H_6O-C_4H_4-C_3H_6O]^-$. By comparison with the previous study (Zheng *et al*., 2020), the compound was identified as 17-hydroxylinolenic acid. Compounds 79 and 80 had retention time of 15.96 min and 16.31 min with the precise molecular formula $C_{32}H_{60}O_{16}$, both showed a quasi-molecular ion at *m/z* 699.381 $[M-H]^-$ and the same fragment ions at *m/z* 415.1460, 397.1352 and 235.0935 corresponding to $[M-H-oleic\ acid]^-$, $[M-H-oleic\ acid-H_2O]^-$ and $[M-H-oleic\ acid-H_2O-glc]^-$. It is speculated that they were isomers of palmitic-oleic glucoside based on the literature (Pierson *et al*., 2014).

Peak 73 was recorded at 14.97 min and yielded the $[M-H]^-$ ion at *m/z* 721.3660. Peak 74 was found at 15.26 min and generated $[M-H]^-$ ion at *m/z* 697.3652. Peak 76 was found at 15.60 min and generated $[M-H]^-$ ion at *m/z* 723.3808. These three compounds shared the same fragmentation pattern and fragment ions at *m/z* 415.146 and 235.082, which were inferred as palmitoleic-linolenic glucoside, palmitoleic-oleic glucoside and palmitoleic-linoleic glucoside by comparison with the literature (Pierson *et al*., 2014).

Alkaloids

The peak time for compound 10 was 1.82 min and the precise molecular formula was $C_{17}H_{31}N_3O_2$, yielding a quasi-ionic peak 310.2486 $[M+H]^+$, yielding fragment ions at *m/z* 179.0847, 171.1490, 292.2378, 84.0814, 98.0968 and was tentatively identified as a palustrine based on the literature (Cramer *et al*., 2015).

The elution of peak 5 resulted in a $[M+H]^+$ ion at *m/z* 144.1258, with the observation of further characteristic fragment ions at *m/z* 84.0815 $[M+H-C_2H_4O_2]^+$, 71.0497 $[M+H-C_3H_7ON]^+$, 58.0660 $[M+H-C_4H_6O_2]^+$ and 55.0587 $[M+H-C_4H_{11}ON]^+$. By comparing with the previous report (Li *et al*., 2023), the compound was identified as stachydrine.

Coumarins

Compound 19 showed an $[M-H]^-$ at *m/z* 339.0721, a fragment ion at m/z 177.0185 ([M-H-CO2]−) and a retention time of 3.74 min, and was putatively identified as esculin based on the database.

Peak 25 was detected at 4.51 min and with a $[M+H]^+$ species at *m/z* 409.1470. MS/MS ions at *m/z* 247.0938 and 229.0839 were consistent with $[M+H-glc]^+$ and $[M+H-glc-H_2O]^+$. Compound 25 was tentatively assigned as nodakenin based on database matching.

Peak 31 eluted at 5.01 min, yielding a protonated molecular ion at *m/z* 177.0546. Subsequent MS/MS fragments at *m/z* 145.0285 and 117.0339 corresponded to losses of O_2 and O_2+CO, respectively. Based on database comparison, this peak was putatively identified as 6-Hydroxy-4-methylcoumarin.

Terpenoids

A total of 10 terpenoids were identified in EH. In mass spectrometry analysis, terpenoids are often prone to losing methyl ions ($-CH_3$) in a single molecule. This is because terpenoids typically contain multiple methyl groups, which are prone to cleavage in mass spectrometry, resulting in the loss of methyl ions in the molecule.

The retention times of compounds 32, 43, 50 and 58 were 5.17 min, 5.93 min, 6.56 and 7.34 min, respectively, with the exact molecular formula $C_{13}H_{20}O$. All yielded quasi-ionic peaks 193.158 $[M+H]^+$ and secondary fragment ions *m/z* 175.1482 $[M+H-H_2O]^+$, 147.1169 $[M+H-H_2O-CO_2]^+$, which, in conjunction with literature reports (Mein *et al*., 2011), are presumed to be the ionone isomers.

The peak times for compounds 42, 53, 59 and 62 were 5.93 min, 6.71 min, 7.36 min and 8.07 min, respectively, with the accurate molecular formula $C_{13}H_{20}O_2$, each showing an $[M+H]^+$ at *m/z* 209.153 with fragments at *m/z* 151.1117 $[M+H-C_3H_6O]^+$, 137.0956 $[M+H-C_4H_8O]^+$, 121.1015 $[M+H-C_4H_8O_2]^+$ and 107.0859 $[M+H-C_5H_{10}O_2]^+$. These were presumed to be isomers of hydroxy-ionone in combination with those reported in the literature at (Luetragoon *et al*., 2020; Mein *et al*., 2011), respectively.

Peak 78 yielded a protonated molecular ion $[M+H]^+$ at *m/z* 219.1744, alongwith characteristic fragment ions detected at *m/z* 203.1431 $[M+H-CH_3]^+$ and 71.0497 $[M+H-CH_3\text{-ara}]^+$. Based on the previous report (Li *et al*., 2023), the compound was identified as α-Cyperone.

Peak 82 was recorded at 23.46 min and generated $[M+H]^+$ ion at *m/z* 425.3785. Characteristic fragment ions at *m/z* 177.1639, 95.0816 and 81.0706 corresponded to $[M+H-C_{17}H_{28}O]^+$, $[M+H-C_{17}H_{28}O-C_6H_{10}]^+$ and $[M+H-C_{17}H_{28}O-C_6H_{10}-CH_2]^+$. Compound 80 was tentatively assigned to lupenone based on a match with the in-house database.

Other compounds

Compounds 36, 39 and 54 eluted at 5.36 min, 5.63 min and 6.99 min, respectively, each showing a precursor ion at *m/z* 197.117 $[M+H]^+$ with fragment ions at *m/z* 179.1067, 135.1169, 161.0961, 113.9640, 107.0859 and were presumed to be an isomer of loliolide (Shi *et al*., 2012).

The retention time of peak 52 was 6.59 min and the quasi-molecular ion at *m/z* 525.1582 $[M+H]^+$, yielding fragment ions at *m/z* 439.1580 $[M+H-C_3H_2O_3]^+$ and 277.1047 $[M+H-C_3H_2O_3\text{-glc}]^+$, which was presumed to be it is 3'-O-(6"-O-malonyl)-glucosylhamaudol (Zolboo, 2020).

Compound 81 was detected a deprotonated ion at *m/z* 279.2330 $[M-H]^-$ and a fragment ion at *m/z* 261.2216 $[M-H-H_2O]^-$ at a retention time of 20.31 min, tentatively assigning it as linoleic acid through database comparison.

DISCUSSION

Natural herbal medicines usually contain structurally diverse metabolites with wide concentration ranges, making comprehensive chemical profiling particularly challenging (Hao *et al*., 2025; Waris *et al*., 2022). Traditional phytochemical investigations of EH have mainly focused on several flavonoids and phenolic acids, while systematic characterization of minor constituents has remained limited (Ma and Zhou, 2025; Zhang *et al*., 2025). In this work, the superior resolving capability, precise mass measurement and high sensitivity of UHPLC-Q-Exactive Orbitrap MS enabled accurate determination of precursor ions and fragment ions, thereby significantly improving the reliability of compound identification. Moreover, the combined acquisition strategy of full MS/dd-MS^2 and PRM effectively compensated for the limitations of conventional data-dependent acquisition, especially for low-abundance compounds that are easily overlooked during automatic fragmentation selection. The incorporation of an inclusion ion list further enhanced the coverage and detection sensitivity for target constituents, enabling more comprehensive MS/MS data acquisition.

Organic acids were the largest category identified in EH, comprising 34 compounds. These compounds mainly included phenolic acids and related derivatives, which are often considered important contributors to antioxidant, anti-inflammatory and diuretic activities in medicinal plants (Saleem *et al*., 2022). The abundant presence of organic acids may therefore partially explain the traditional medicinal functions of EH, particularly its heat-clearing and diuretic effects (Baptista *et al*., 2024; Xie *et al*., 2024). In addition, 22 flavonoids were characterized in this study. Flavonoids are widely recognized as major bioactive constituents in many medicinal herbs and exhibit multiple biological activities, such as antioxidative, anti-inflammatory, antimicrobial and vasoprotective properties (Liu *et al*., 2025; Mutha *et al*., 2021; Pallag *et al*., 2016). Previous studies on EH have primarily emphasized flavonoid constituents, however, the present work further expanded the number of flavonoids identified in EH to a certain extent and revealed a broader structural diversity than previously recognized. Interestingly, 10 terpenes were also identified in EH. Studies have shown that terpenoids are capable of downregulating pro-inflammatory cytokine production, including TNF-α and IL-6 and also display antimicrobial activity against a range of pathogenic microorganisms, such as Staphylococcus aureus, Escherichia coli and Candida albicans (Devi *et al*., 2024; Trepa *et al*., 2024). In addition, several amino acids, nucleotides, coumarins and alkaloids were detected, indicating that EH contains multiple classes of primary and secondary metabolites that may collectively contribute to its therapeutic effects through synergistic interactions.

Compared with conventional phytochemical separation methods, the analytical strategy established herein demonstrated clear advantages in analytical throughput, detection sensitivity and overall constituent coverage. The use of UHPLC significantly shortened analysis time while

maintaining satisfactory chromatographic resolution (Geng *et al*., 2021; Li *et al*., 2026). Furthermore, Orbitrap high-resolution mass spectrometry provided accurate mass measurements with excellent selectivity, enabling efficient compound identification even in highly complex matrices (Zhu *et al*., 2022). Therefore, this strategy may serve as a practical and efficient approach for rapid chemical profiling and quality evaluation of EH and other traditional herbal medicines. Nevertheless, several limitations still exist in the present study. Most compounds were preliminarily characterized through precise mass measurements, characteristic MS/MS fragmentation behaviors, reference standards and database matching, while some constituents still require further structural confirmation by isolation and nuclear magnetic resonance (NMR) analysis (Geng *et al*., 2021; Hu *et al*., 2021). Additionally, although comprehensive chemical profiling was achieved, the correlations between these constituents and the pharmacological effects of EH remain unclear. Future studies should therefore focus on quantitative analysis, bioactivity evaluation, metabolomic investigation and pharmacodynamic correlation analysis to clarify the active material basis and mechanisms of action of EH (Huang *et al*., 2021).

CONCLUSION

An effective and rapid analytical approach was established using a UHPLC-Q-Exactive Orbitrap MS, with full MS scans followed by PRM with an inclusion ion list, for the systematic qualitative profiling of chemical constituents in EH. A total of 82 compounds were identified or tentatively characterized, including 34 organic acids, 22 flavonoids, 10 terpenes and other minor constituents, among which 71 compounds were reported in EH for the first time. These findings systematically expanded the current understanding of the chemical profile of EH. Moreover, the established analytical strategy provides an effective approach for the rapid characterization of chemical constituents in EH and related traditional Chinese medicines and offers a theoretical basis for further studies of their pharmacodynamic mechanisms.

Acknowledgments
None.

Author's contributions
Qing Li: Writing—original draft, investigation and data curation; Pei Xiong: Conceptualization, formal analysis and validation; Ming Zhang: Data curation, investigation and formal analysis; Kaiquan Yu: Resources; Jiaxin Li: Software; Hui Li: Writing—review and editing, conceptualization, supervision and conceptualization. All authors read and agreed to the published version of the manuscript.

Funding
There was no funding.

Data availability statement
The datasets generated during and/or analysed during the current study are available from the corresponding author on reasonable request.

Ethical approval
Not applicable.

Conflict of interest
The authors declare no conflicts of interest.

Supplementary data
https://pjps.pk/uploads/2026/08/SUP1787724972.pdf

REFERENCES

Ataseven S, Misirli D, Uzar F, Türkan NN and Elmastas M (2021). Determination of phenolic compound composition of water and ethanol extracts of horsetail (Equisetum arvense). *Bütünleyici ve Anadolu Tıbbı Dergisi*, **2**(2): 3-9.

Baptista F, PaieRibeiro J, Almeida M and Barros AN (2024). Exploring the role of phenolic compounds in chronic kidney disease: A systematic review. *Molecules*, **29**(11): 2576.

Boeing T, Tafarelo Moreno KG, Gasparotto Junior A, Mota da Silva L and De Souza P (2021). Phytochemistry and pharmacology of the genus Equisetum (Equisetaceae): A narrative review of the species with therapeutic potential for kidney diseases. *Evid. Based Complement. Alternat. Med.*, **2021**(1): 6658434.

Bowie JH, Brinkworth CS and Dua S (2002). Collision-induced fragmentations of the (M-H)- parent anions of underivatized peptides: An aid to structure determination and some unusual negative ion cleavages. *Mass Spectrom. Rev.*, **21**(2): 87-107.

Cai W, Li KL, Xiong P, Gong KY, Zhu L, Yang JB and Wu WH (2020). A systematic strategy for rapid identification of chlorogenic acids derivatives in Duhaldea nervosa using UHPLC-Q-Exactive Orbitrap mass spectrometry. *Arab. J. Chem.*, **13**(2): 3751-3761.

Chen YJ, Wu H, Wei ZY, Chen LM and Dong JJ (2019). Identification of chemical constituents in Aster tataricus by UHPLC-Q-TOF-MS. *Acta. Pharm. Sin. B.*, **12**: 1645-1654.

Chinese Pharmacopoeia Commission (2025). Pharmacopoeia of the People's Republic of China, Part 1 edn, China Medical Science Press, Beijing, p. **66**.

Choi SS, Song MJ, Kim OB and Kim Y (2013). Fragmentation patterns of protonated amino acids formed by atmospheric pressure chemical ionization. *Rapid Commun Mass Spectrom*, **27**(1): 143-151.

Cramer L, Ernst L, Lubienski M, Papke U, Schiebel HM,

Jerz G, Beuerle T (2015). Structural and quantitative analysis of Equisetum alkaloids. *Phytochemistry*, **116**: 269-282.

Devi M, Bamrah PK, Goyal R, Choudhary M, Chopra H (2024). Insights on the emerging therapeutic potential of terpenoids as anti-inflammatory agents: A scoping review. *J. Bio-X Res.*, **7**: 0006.

Dong X and Huang R (2022). Ferulic acid: An extraordinarily neuroprotective phenolic acid with anti-depressive properties. *Phytomedicine*, **105**: 154355-154355.

Editorial Committee of flora of China (2004). Flora of China, **6**: Science Press, Beijing, p. 238.

Geng JL, Xiao LH, Chen C, Wang ZZ, Xiao W and Wang QH (2021). An integrated analytical approach based on enhanced fragment ions interrogation and modified Kendrick mass defect filter data mining for in-depth chemical profiling of glucosinolates by ultra-high-pressure liquid chromatography coupled with Orbitrap high resolution mass spectrometry. *J. Chromatogr. A.*, **1639**: 461903-.

Guijarro-Diez M, Nozal L, Marina ML and Crego AL (2015). Metabolomic fingerprinting of saffron by LC/MS: Novel authenticity markers. *Anal. Bioanal. Chem.*, **407**: 7197-7213.

Hao YC, Zhang ZH, Luo EX, Yang J and Wang SC (2025). Plant metabolomics: Applications and challenges in the era of multi-omics big data. *Abiotech*, **6**(1): 116-132.

He M, Wu H, Nie J, Yan P, Yang TB, Yang ZY and Pei R (2017). Accurate recognition and feature qualify for flavonoid extracts from Liang-wai Gan Cao by liquid chromatography-high resolution-mass spectrometry and computational MS/MS fragmentation. *J. Pharm. Biomed. Anal.*, **146**: 37-47.

Hu HB, Hu CL, Peng JN, Ghosh AK, Khan A, Sun D and Luyten W (2021). Bioassay-Guided interpretation of antimicrobial compounds in Kumu, a TCM preparation from picrasma quassioides' Stem via UHPLC-Orbitrap-Ion trap mass spectrometry combined with fragmentation and retention time calculation. *Front. Pharmacol.*, **12**: 761751.

Hu QY, Tang HR and Wang YL (2020). Challenges in analysis of hydrophilic metabolites using chromatography coupled with mass spectrometry. *J. Anal. Test*, **4**: 140-162.

Huang WW, Zhang ZL, Niu L, Hu XH, Teka T, Han LF, Pan GX and Wang QL (2021). Rapid discovery of potentially vasodilative compounds from Uncaria by UHPLC/Q-Orbitrap-MS based metabolomics and correlation analysis. *J. Pharm. Biomed. Anal.*, **206**: 114384.

Jaiswal R, Jayasinghe L and Kuhnert N (2012). Identification and characterization of proanthocyanidins of 16 members of the Rhododendron genus (Ericaceae) by tandem LC–MS. *J. Mass. Spectrom.*, **47**(4): 502-515.

Jiang C and Gates PJ (2024). Systematic characterisation of the fragmentation of flavonoids using high-resolution accurate mass electrospray tandem mass spectrometry. *Molecules*, **29**(22): 5246.

Jiang YL, Wu F, Huang F, Wu HQ and Huang XL (2018). Simultaneous determination of 6 flavonoids in hawthorn by high performance liquid chromatography-tandem mass spectrometry. *Chin. J. Pharm. Anal.*, **38**(7): 1139-1145.

Li JX, Zou SQ, Yang WL, Peng MD, Chen BZ, Deng JJ, Wei MY and Zheng GD (2023). Identification of volatile and nonvolatile compounds in citri reticulatae pericarpium viride using GC-MS, UPLC-Q-Exactive Orbitrap-MS and HPLC-PDA. *Food Sci. Nutr.*, **11**(3): 1415-1425.

Li KL, Wu P, Li SY, Huang YL, Wang L, Chen YF, Zou YF, Yan F and Cai W (2024). An integrated strategy for comprehensive characterization of chemical components in Qingqiao Kangdu granules by UHPLC-Q-Exactive-MS coupled with feature-based molecular networking. *Arab. J. Chem.*, **17**(1):105463.

Li Q, Li KL, Yang JT, Cai W, Yang HQ, Gao BW and Cai W (2026). Rapid identification of chemical components in polygonatum kingianum Collett & Hemsl. BASED on UHPLC-Q-Exactive orbitrap MS coupled with molecular networking. *J. Chromatogr. B*: 124943.

Liao XY, Hong Y and Chen ZL (2021). Identification and quantification of the bioactive components in Osmanthus fragrans roots by HPLC-MS/MS. *J. Pharm. Anal.*, **11**(3): 299-307.

Liu Y, Zhu JJ, Liu ZY, Zhi Y, Mei C and Wang HJ (2025). Flavonoids as promising natural compounds for combating bacterial infections. *Int. J. Mol. Sci.*, **26**(6): 2455-2455.

Luetragoon T, Pankla Sranujit R, Noysang C, Thongsri Y, Potup P, Suphrom N, Nuengchamnong N and Usuwanthim K (2020). Bioactive compounds in Moringa oleifera Lam. leaves inhibit the pro-inflammatory mediators in lipopolysaccharide-induced human monocyte-derived macrophages. *Molecules*, **25**(1): 191.

Luo X, Liao YH, Qing T, Zhao JH and Cai W (2026). Rapid analysis of the chemical composition of Xiaoban Kangfu capsules based on UHPLC-Q-Exactive Orbitrap MS/MS combined with molecular networks. *Pharmaceuticals*, **19**(3): 459.

Ma Y and Zhou Z (2025). Research progress on chemical constituents, pharmacological effects and clinical application of *Equisetum hyemale*. *Northwest Pharm J*, **40**(1): 46-61.

Ma YB, Wang CL, Wang FX, Wang M, Tian W, Wu LF and Niu LY (2022). Rapid identification of chemical components of Folium Photiniae based on UPLC-Q-TOF-MS. *Chin Tradit Herb Drugs*, **53**(20): 6401-6411.

Mein JR, Dolnikowski GG, Ernst H, Russell RM and Wang XD (2011). Enzymatic formation of apo-

carotenoids from the xanthophyll carotenoids lutein, zeaxanthin and β-cryptoxanthin by ferret carotene-9′, 10′-monooxygenase. *Arch. Biochem. Biophys.*, **506**(1): 109-121.

Mutha RE, Tatiya AU and Surana SJ (2021). Flavonoids as natural phenolic compounds and their role in therapeutics: An overview. *Future J Pharm Sci*, **7**(1): 25-25.

Nicolau dQL, Carvalho DFAC, Freimann WG, Dutra dSDP, Fagundes PACR, Frankland SACH, Paes dAEC, Sergio dAB, Davyson dLM and Kaufmann RB (2023). New substances of Equisetum hyemale L. extracts and their *in-vivo* antitumoral effect against oral squamous cell carcinoma. *J Ethnopharmacol*, **303**: 116043-116043.

Onozato M, Kanda R, Sato Y, Sakamoto T, Umino M and Fukushima T (2022). Column-switching high-performance liquid chromatography-fluorescence detection method for malic acid enantiomers in commercial wines. *J Food Compos Anal*, **106**: 104282.

Pallag A, Bungau S, Tit DM, Jurca T, Sirbu V, Honiges A, Horhogea C (2016). Comparative study of polyphenols, flavonoids and chlorophylls in equisetum arvense L. populations. *Rev Chim*, **67**(3): 530-533.

Pierson JT, Monteith GR, Roberts Thomson SJ, Dietzgen RG, Gidley MJ, Shaw PN (2014). Phytochemical extraction, characterisation and comparative distribution across four mango (Mangifera indica L.) fruit varieties. *Food Chem*, **149**:253-263.

Ren TK, Li ML, Zheng H, Wang Z, Zhang JL (2020). Characterization of acidic glycosphingolipid changes in C6 glioma rats treated with temozolomide using ultra-high-performance liquid chromatography coupled with quadrupole time-of-flight mass spectrometry. *J Anal Test*, **4**: 217-225.

Saleem A, Akhtar MF, Sharif A, Akhtar B, Siddique R, Ashraf GM, Alghamdi BS, Alharthy SA (2022). Anticancer, cardio-protective and anti-inflammatory potential of natural-sources-derived phenolic acids. *Molecules*, **27**(21): 7286.

Sánchez-Rabaneda F, Jauregui O, Lamuela-Raventos RM, Viladomat F, Bastida J and Codina C (2004). Qualitative analysis of phenolic compounds in apple pomace using liquid chromatography coupled to mass spectrometry in tandem mode. *Rapid Commun Mass Sp*, **18**(5): 553-563.

Shi YY, Guan SH, Tang RN, Tao SJ and Guo DA (2012). Simultaneous determination of atractylenolide II and atractylenolide III by liquid chromatography–tandem mass spectrometry in rat plasma and its application in a pharmacokinetic study after oral administration of Atractylodes Macrocephala Rhizoma extract. *Biomed Chromatogr*, **26**(11): 1386-1392.

Shu LY, Xiao SL, Li KL, Luo HB, Li M, Yang QR, Gao BW, Li JX, Yan F and Cai W (2025). Systematic identification of the chemical components of leaves and roots of Didymocarpus heucherifolius Hand.-Mazz. based on UHPLC Q-Exactive Orbitrap MS technology coupled with molecular networking strategy. *Sci Rep*, **15**(1): 2617.

Sun HY, Liu MX, Lin ZT, Jiang HX, Niu YY, Wang H, Chen SZ (2015). Comprehensive identification of 125 multifarious constituents in Shuang–huang–lian powder injection by HPLC-DAD-ESI-IT-TOF-MS. *J Pharm Biomed Anal*, **115**: 86-106.

Trepa M, Sulkowska Ziaja K, Kala K, Muszynska B (2024). Therapeutic potential of fungal terpenes and terpenoids: Application in skin diseases. *Molecules*, **29**(5):1183.

Wang L, Tan NN, Wang H, Hu JB, Diwu WB, Wang XL (2020). A systematic analysis of natural α-glucosidase inhibitors from flavonoids of Radix scutellariae using ultrafiltration UPLC-TripleTOF-MS/MS and network pharmacology. *Bmc Complement Med Ter*, **20**:1-17.

Wang SM, Li X, Chen BX, Li ST, Wang JL, Wang J, Yang MS, Xu XY, Wang HD, Yang WZ (2022). Dimension-enhanced ultra-high performance liquid chromatography/ion mobility-quadrupole time-of-flight mass spectrometry combined with intelligent peak annotation for the rapid characterization of the multiple components from seeds of Descurainia sophia. *Phyton*, **91**(3):541.

Wang XL, Peng MM, Chen Q, Me X and He TY (2023). Identification of chemical components and network pharmacology of Huanglian Decoction based on UPLC-Q-TOF-MS /MS technology. *China J Chin Mater Med*, **48**(5):1249-1263.

Waris M, Kocak E, Gonulalan EM, Demirezer LO, Kır S and Nemutlu E (2022). Metabolomics analysis insight into medicinal plant science. *TrAC Trends in Analytical Chemistry*, **157**:116795.

Wilfried MAN and Ricardo ACC (2017). Interpretation of MS-MS mass spectra of drugs and pesticides. *Anal Bioanal Chem*, **409**(30): 6935-6936.

Wu D, Cui M, Hao YB, Liu LH, Zhou YL, Wang WJ, Xue AH, Chingin K and Luo LP (2019). In situ study of metabolic response of Arabidopsis thaliana leaves to salt stress by neutral desorption-extractive electrospray ionization mass spectrometry. *J Agric Food Chem*, **67**(46): 12945-12952.

Wu TT, Zhao P, Lyu ZG, Ouyang HZ, He J (2025). Quality evaluation of *Equisetum hyemale* L. by UPLC fingerprint and multi-component quantification. *J Tianjin Univ Tradit Chin Med*, **44**(25):404-409.

Xie GY, Zhu Y, Shu P, Qin XY, Wu G, Wang Q, Qin MJ (2014). Phenolic metabolite profiles and antioxidants assay of three Iridaceae medicinal plants for traditional Chinese medicine “She-gan” by on-line HPLC–DAD coupled with chemiluminescence (CL) and ESI-Q-TOF-MS/MS. *J Pharm Biomed Anal*, **98**:40-51.

Xie JC, Xiong SH, Li YM, Xia BH, Li MJ, Zhang ZM, Shi Z, Peng QX, Li C, Lin LM (2024). Phenolic acids from medicinal and edible homologous plants: A potential anti-inflammatory agent for inflammatory

diseases. *Front Immunol*, **15**: 1345002.

Xiong H, Li N, Yu YZ, Liu Z, Li Z and Zhao L (2023). Comprehensive Characterization and identification of chemical constituents of Xiangsha Pingwei Pills by UPLC–Q-TOF-MS. *J AOAC Int*, **106**(4): 1017-1036.

Yang X, Cui XX, Zhao L, Guo D, Feng L, Wei S, Zhao C and Huang D (2017). Exogenous glycine nitrogen enhances accumulation of glycosylated flavonoids and antioxidant activity in lettuce (*Lactuca sativa L.*). *Front Plant Sci*, **8**: 2098.

Zhang B, Li Y, Jiang L, Liu J, Ma X, Zhao S and Sun X (2025). Identification of chemical constituents in *Equisetum hyemale* L. based on UPLC-Q-Exactive-Plus-Orbitrap-MS. *Chem Reagents*, **47**(4): 94-104.

Zhang LY, Qin SH, Tang SN, E S, Li KL, Li J, Cai W, Sun L and Li H (2022). Qualitative analysis of multiple phytochemical compounds in tojapride based on UHPLC Q-exactive orbitrap mass spectrometry. *Molecules*, **27**(19): 6639.

Zhang M, Li Q, Yu KQ, Li JX, Wu JL, Li SN, Chen YQ, Cai W and Ma JY (2023). Systemic chemical characterization of Lemna minor by UHPLC-Q-Exactive Orbitrap MS coupled with parallel reaction monitoring. *J Mass Spectrom*, **58**(6): e4923.

Zheng YF, Li DY, Sun J, Cheng JM, Chai C, Zhang L and Peng GP (2020). Comprehensive comparison of two color varieties of perillae folium using rapid resolution liquid chromatography coupled with quadruple-time-of-flight mass spectrometry (RRLC-Q/TOF-MS)-based metabolic profile and *in-vivo*/*in-vitro* anti-oxidative activity. *J Agric Food Chem*, **68**(49): 14684-14697.

Zhu L, Ma SJ, Li KL, Xiong P, Qin SH and Cai W (2022). Systematic screening of chemical constituents in the traditional Chinese medicine arnebiae radix by UHPLC-Q-Exactive orbitrap mass spectrometry. *Molecules*, **27**(9): 2631.

Batsukh Z (2020). Characterization of metabolites in Mongolian Saposhnikovia divaricata roots by means of various analytical methods (Doctoral dissertation, University of Toyama).